HHS Public Access

Author manuscript

Proc SPIE Int Soc Opt Eng. Author manuscript; available in PMC 2018 July 19.

Published in final edited form as:

Proc SPIE Int Soc Opt Eng. 2018 February ; 10473: . doi:10.1117/12.2296023.

Lesion Dehydration Rate Changes with the Surface Layer Thickness during Enamel Remineralization

Nai-Yuan N. Chang, **Jamison M. Jew**, and **Daniel Fried**

University of California, San Francisco, San Francisco, CA 94143-0758, U.S.A

Abstract

A transparent highly mineralized outer surface zone is formed on caries lesions during remineralization that reduces the permeability to water and plaque generated acids. However, it has not been established how thick the surface zone should be to inhibit the penetration of these fluids. Near-IR (NIR) reflectance coupled with dehydration can be used to measure changes in the fluid permeability of lesions in enamel and dentin. Based on our previous studies, we postulate that there is a strong correlation between the surface layer thickness and the rate of dehydration. In this study, the rates of dehydration for simulated lesions in enamel with varying remineralization durations were measured. Reflectance imaging at NIR wavelengths from 1400–2300 nm, which coincides with higher water absorption and manifests the greatest sensitivity to contrast changes during dehydration measurements, was used to image simulated enamel lesions. The results suggest that the relationship between surface zone thickness and lesion permeability is highly non-linear, and that a small increase in the surface layer thickness may lead to a significant decrease in permeability.

Keywords

dental caries; NIR reflectance imaging; lesion dehydration; lesion permeability

1. INTRODUCTION

The nature of the caries problem has changed dramatically. The majority of newly discovered carious lesions are highly localized to the occlusal pits and fissures of the posterior dentition and the proximal contact sites between teeth, where they are more difficult to detect. Clinicians mostly rely on palpation and visual inspection to discern whether dental decay is active or arrested [1]. If the lesion appears dark, smooth, and hard, they would likely decide that the lesion is arrested [2]. However, this method is subjective and unreliable. Many lesions have been arrested or do not require intervention. Even so, it is difficult to identify active lesions with current diagnostic methods. Accurate assessment of lesion activity, depth, and severity is important to determine whether intervention is necessary. Effective employment of new optical diagnostic technologies that can exploit the changes in the light scattering of the lesion have great potential for diagnosing the present state of the lesions. Therefore, the development of new methods, such as NIR reflectance dehydration imaging, are needed for the clinical assessment of lesion activity and to avoid unnecessary cavity preparations.

When lesions become arrested by mineral deposition, or remineralization, in the outer layers of the lesion, the diffusion of fluids into the lesion is inhibited. Hence, the rate of water diffusion out of the lesion reflects the degree of lesion activity. Previous studies have demonstrated that the optical changes due to the loss of water from porous lesions can be exploited to assess lesion severity and activity with QLF, thermal, and SWIR imaging [3–9]. Since arrested lesions and developmental defects (fluorosis) are less permeable to water due to the highly mineralized surface layer, changes in the rate of water loss can be related to changes in lesion structure and porosity. We have investigated optical methods for assessing water diffusion rates from lesions since the porosity of the outer layers of active lesions is significantly greater than arrested lesions. This can be indirectly measured via NIR reflectance methods [10–12]. Normal enamel is transparent in NIR wavelengths, whereas early demineralization causes increased NIR reflectance due to scattering. Water in the pores at the surface of the lesion absorbs the incident NIR light, particularly at wavelengths such as 1450 nm, reducing surface scattering and lesion contrast. Loss of that water during dehydration produces a marked increase in reflectivity and lesion contrast.

New technologies are also needed to determine whether lesions are active and expanding, partially arrested and undergoing remineralization, or fully arrested and remineralized. Polarization Sensitive-Optical Coherence Tomography (PS-OCT) using NIR light is capable of this task since it provides a measure of the reflectivity from each layer of the lesion and is able to detect the formation of a zone of increased mineral density and reduced light scattering due to remineralization. Arrested lesions exhibit a well-defined surface zone of reduced reflectivity that can be clearly resolved in OCT images [13–15].

The purpose of this study is to develop a method to assess lesion activity. We hypothesize that the thickness of the highly mineralized transparent surface zone formed during remineralization correlates with the lesion permeability and activity in enamel. Here, we correlate the results from NIR reflectance dehydration measurements and PS-OCT measurements and found that minor changes in surface layer thickness may lead to major changes in fluid permeability in remineralized enamel lesions. The results here will be confirmed by histology using polarized light microscopy (PLM) and transverse microradiography (TMR).

2. MATERIALS AND METHODS

2.1 Sample Block Preparation

Enamel blocks (n=20), approximately 10–12 mm in length with a width of 2 mm and a thickness of 2 mm, were prepared from extracted bovine incisors acquired from a slaughterhouse. Enamel blocks were ground to a 9 μm finish. Figure 1 shows the workflow of the study design employed.

2.2 Demineralization and Remineralization

A thin layer of acid-resistant varnish in the form of nail polish, Revlon 270 (New York, NY), was applied to all sides except the non-control top surfaces of the enamel blocks before exposure to the demineralization solution. Samples were immersed in 40 mL aliquots of the

demineralization solution for 24 hours. The demineralization solution, which was maintained at 37°C and pH 4.8, was composed of 2.0 mmol/L calcium, 2.0 mmol/L phosphate, and 75 mmol/L acetate. This dissolution model is a "surface softened" dissolution model designed to produce subsurface dissolution while maintaining an intact surface, and it simulates highly active early lesions of approximately 100–200 μm thick on the surface. A demineralized surface is then covered with the same acid-resistant varnish, where the rest of the samples were exposed to an acidic remineralization regimen for varying duration (see Figure 1). The acidic remineralization model has been successful in increasing mineralization of the lesion body [16]. The acidic remineralization solution was composed of 4.1 mmol/L calcium, 15 mmol/L phosphate, 50 mmol/L lactic acid, 20 mmol/L HEPES buffer, and 2 ppm F- maintained at 37°C and a pH of 4.8 [16]. After each time point of remineralization, beginning at 0 hour of remineralization, NIR reflectance dehydration and PS-OCT measurements were recorded.

2.3 Near-IR Dehydration Measurements

Each sample was placed in a mount connected to a high-speed XY-scanning motion controller system (Newport, Irvine, CA) ESP301 controller and 850G-HS stages, coupled with an air nozzle and a light source as described in [7]. Each sample was immersed in the water bath for 30 seconds while being vigorously shaken to enhance water diffusion. After the sample was removed from the water bath, an image was captured as an initial reference image and the air spray was activated. The air pressure was set to 15 psi and the computer-controlled air nozzle was positioned 5 cm away from the sample. Each measurement consisted of capturing a sequence of images at 4 frames per second for 60 seconds. The dehydration setup was completely automated using LabVIEW software (National Instruments, Austin, TX).

A Xeva-2.35-320 SWIR T2SL camera (Xenics, Leuven, Belgium) with response up to wavelength of 2.35 μm was used to acquire all the images during the dehydration process. Light from a 150 W fiber-optic illuminator FOI-1 (E Licht Company, Denver, CO) was directed at the sample at an incident angle of approximately 60° to reduce specular reflection and the source to sample distance was fixed at 5 cm. A FEL LP series long-pass filter at 1500 nm (Thorlabs, Newton, NJ) was used. NIR reflectance images were processed and automatically analyzed using a dedicated program constructed with LabVIEW software. A region of interest (ROI) encompassing the whole sample was used and measurement was recorded for each time point. The intensity difference between the final and initial images, $\Delta I_{(t=60)}$, was calculated using $I_{60} - I_0$, where I_{60} is the mean intensity at t = 60 seconds and I_0 is the mean intensity prior to turning on the air nozzle.

2.4 Polarization-Sensitive Optical Coherence Tomography (PS-OCT)

An all-fiber-based optical coherence domain reflectometry (OCDR) system with polarization maintaining (PM) optical fiber, high-speed piezoelectric fiber-stretchers, and two balanced InGaAs receivers from Optiphase, Inc., Van Nuys, CA was used. This two-channel system was integrated with a broadband superluminescent diode (SLD) Denselight (Jessup, MD) and a high-speed XY-scanning system, ESP-300 controller and 850G-HS stages from Newport (Irvine, CA) for in vitro optical coherence tomography. This system is

based on a polarization-sensitive Michelson white light interferometer. The high power (15 mW) polarized SLD source operated at a center wavelength of 1317 nm with a spectral bandwidth full-width at half-maximum (FWHM) of 84 nm. The sample arm was coupled to an AR-coated fiber-collimator to produce a collimated beam with a 6-mm diameter. The beam was focused onto the sample surface using a 20-mm focal length AR-coated planoconvex lens. This configuration provided lateral resolution of approximately 20-μm and an axial resolution of 10 μm in air with a signal to noise ratio of greater than 40–50 dB. The PS-OCT system is completely controlled using LabVIEW software. The system is described in greater detail in previous work [17]. Acquired scans are compiled into b-scan files. Image processing was carried out using Igor Pro, data analysis software from Wavemetrics Inc. (Lake Oswego, OR).

We have developed automated methods for determining the lesion depth (LD), the integrated reflectivity over the lesions depth (ΔR), and the thickness of the transparent surface layer (TSL) [18]. ΔR is calculated from the cross-polarization image and it is analogous to the integrated mineral loss with depth. The average LD, ΔR, and TSL values were calculated across all windows.

2.5 Data Analysis

Prism 7 (GraphPad Software Inc., La Jolla, CA) was used for regression.

3. RESULTS AND DISCUSSIONS

3.1 NIR Dehydration Measurements

NIR reflectance dehydration measurements for the samples are shown in Fig. 2. ΔI changes as the duration of remineralization increases and it was highly variable. The dehydration curves exhibited more variation in shape initially, but as remineralization duration increased, the sigmoidal characteristic of the curve stabilized. At 192 hours (8 days) of remineralization, permeability still did not return to baseline (thick black curve), suggesting that further remineralization might be necessary to fully remineralize using this model.

3.2 PS-OCT Measurements

Sample enamel PS-OCT B-scans are shown in Figure 3. As expected, the demineralized zone showed higher ΔR compared to the control zone. As remineralization duration increases, the difference in ΔR between the demineralized zone and the remineralized zone increases. Even though at 192 hours of remineralization the remineralized zone did not fully remineralize, the formation of a thin transparent surface zone was visibly apparent with PS-OCT.

Figure 4 shows the correlation between NIR reflectance dehydration measurement and the thickness of the transparent surface layer measured by PS-OCT by samples. The plot presented a general negative trend of decreasing permeability, or decreasing ΔI, as the thickness of the transparent surface layer increases. However, the variability of permeability was greater when the transparent surface layer was thinner compared to when the transparent layer was thicker. An explanation for this might be the inherent variation of the

enamel structures such as enamel rod orientation, and the rate and location at which minerals are deposited. The remineralization model we have employed here may not penetrate the entire depth of the demineralized zone, as shown in Fig. 3.

In all, the results suggest that the permeability decreased with increasing transparent surface layer thickness. Furthermore, small increases in transparent surface layer thickness of < 20 μm lead to large permeability changes. Histology will be performed to validate the results here to determine the validity of permeability measurements as a method to assess lesion activity.

Acknowledgments

The authors acknowledge the support of NIH/NIDCR Grants F30-DE027264 and R01-DE14698.

References

1. Fejerskov O, , Kidd E. Dental Caries: The Disease and its Clinical Management Blackwell Oxford: 2003
2. Pitts N. Detection, Assessment, Diagnosis and Monitoring of Caries Karger Basel: 2009
3. Kaneko K, , Matsuyama K, , Nakashima S. Early detection of Dental caries II Vol. 4. Indiana University; 1999Quantification of Early Carious Enamel Lesions by using an Infrared Camera; 8399
4. Zakian CM, Taylor AM, Ellwood RP, Pretty IA. Occlusal caries detection by using thermal imaging. J Dent. 2010; 38(10):788–795. [PubMed: 20599464]
5. Usenik P, Bürmen M, Fidler A, Pernuš F, Likar B. Near-infrared hyperspectral imaging of water evaporation dynamics for early detection of incipient caries. J Dent. 2014; 42(10):1242–1247. [PubMed: 25150104]
6. Ando M, Ferreira-Zandona AG, Eckert GJ, Zero DT, Stookey GK. Pilot clinical study to assess caries lesion activity using quantitative light-induced fluorescence during dehydration. J Biomed Opt. 2017; 22(3):35005. [PubMed: 28280839]
7. Lee RC, Darling CL, Fried D. Assessment of remineralization via measurement of dehydration rates with thermal and near-IR reflectance imaging. J Dent. 2015; 43:1032–1042. [PubMed: 25862275]
8. Lee RC, Staninec M, Le O, Fried D. Infrared methods for assessment of the activity of natural enamel caries lesions. IEEE J Selected Top Quant Elect. 2014; 22(3):6803609.
9. Lee RC, Darling CL, Fried D. Activity assessment of root caries lesions with thermal and near-infrared imaging methods. J Biophotonics. 2016; 10(3):433–445. [PubMed: 27060450]
10. Chung S, Fried D, Staninec M, Darling CL. Multispectral near-IR reflectance and transillumination imaging of teeth. Biomed Opt Express. 2011; 2(10):2804–2814. [PubMed: 22025986]
11. Fried WA, Darling CL, Chan K, Fried D. High Contrast Reflectance Imaging of Simulated Lesions on Tooth Occlusal Surfaces at Near-IR Wavelengths. Lasers Surg Med. 2013; 45(8):533–541. [PubMed: 23857066]
12. Simon JC, Chan KH, Darling CL, Fried D. Multispectral near-IR reflectance imaging of simulated early occlusal lesions: variation of lesion contrast with lesion depth and severity. Lasers Surg Med. 2014; 46(3):203–15. [PubMed: 24375543]
13. Kang H, Darling CL, Fried D. Nondestructive monitoring of the repair of enamel artificial lesions by an acidic remineralization model using polarization-sensitive optical coherence tomography. Dent Materials. 2012; 28(5):488–494.
14. Jones RS, Fried D. Remineralization of enamel caries can decrease optical reflectivity. J Dent Res. 2006; 85(9):804–8. [PubMed: 16931861]
15. Jones RS, Darling CL, Featherstone JD, Fried D. Remineralization of in vitro dental caries assessed with polarization-sensitive optical coherence tomography. J Biomed Optics. 2006; 11(1): 014016.

16. Yamazaki H, Margolis HC. Enhanced enamel remineralization under acidic conditions in vitro. J Dent Res. 2008; 87(6):569–74. [PubMed: 18502967]
17. Fried D, Xie J, Shafi S, Featherstone JDB, Breunig T, Lee CQ. Early detection of dental caries and lesion progression with polarization sensitive optical coherence tomography. J Biomed Optics. 2002; 7(4):618–627.
18. Chan KH, Chan AC, Fried WA, Simon JC, Darling CL, Fried D. Use of 2D images of depth and integrated reflectivity to represent the severity of demineralization in cross-polarization optical coherence tomography. J Biophotonics. 2015; 8(1–2):36–45. [PubMed: 24307350]

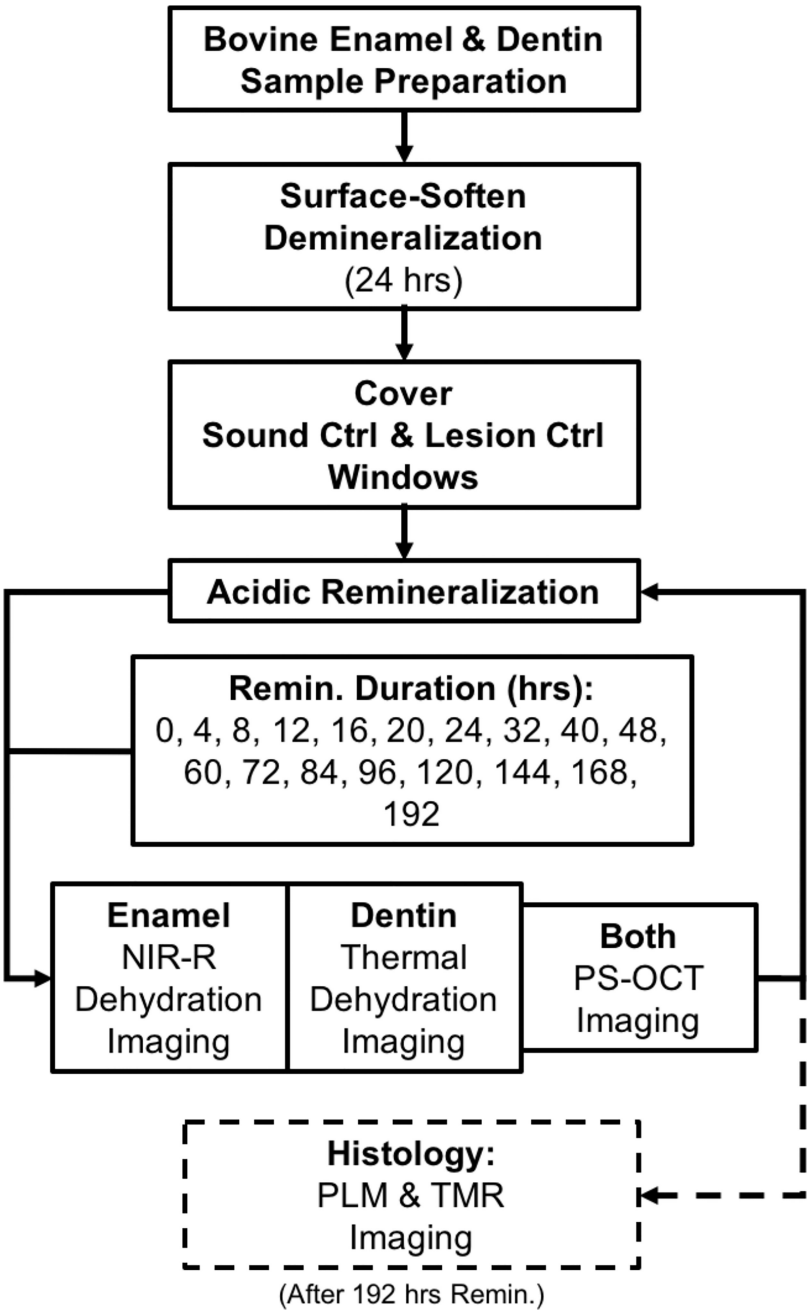

Fig. 1.
Workflow of the experimental setup.

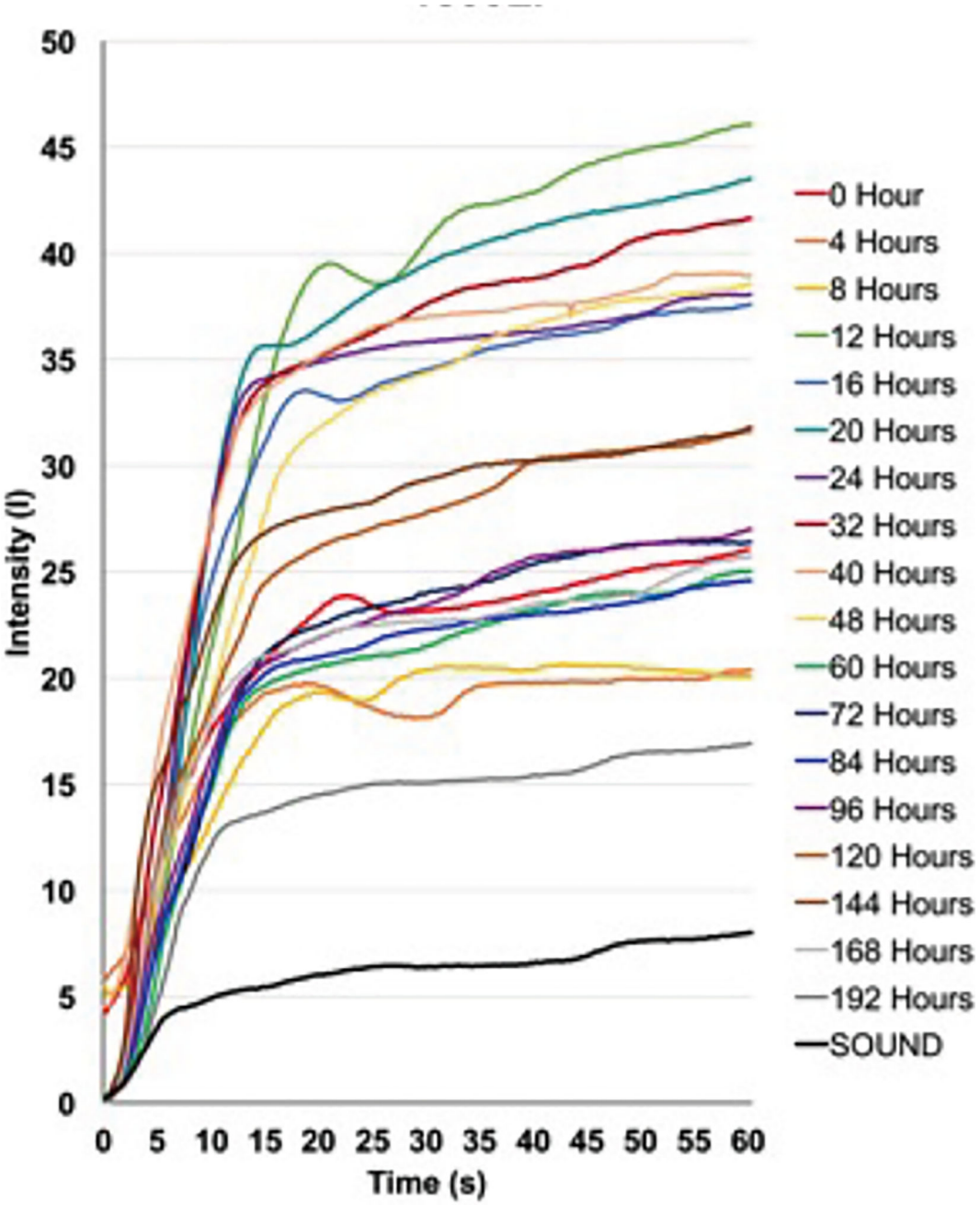

Fig. 2.
Average dehydration curves from 1500–1700-nm.

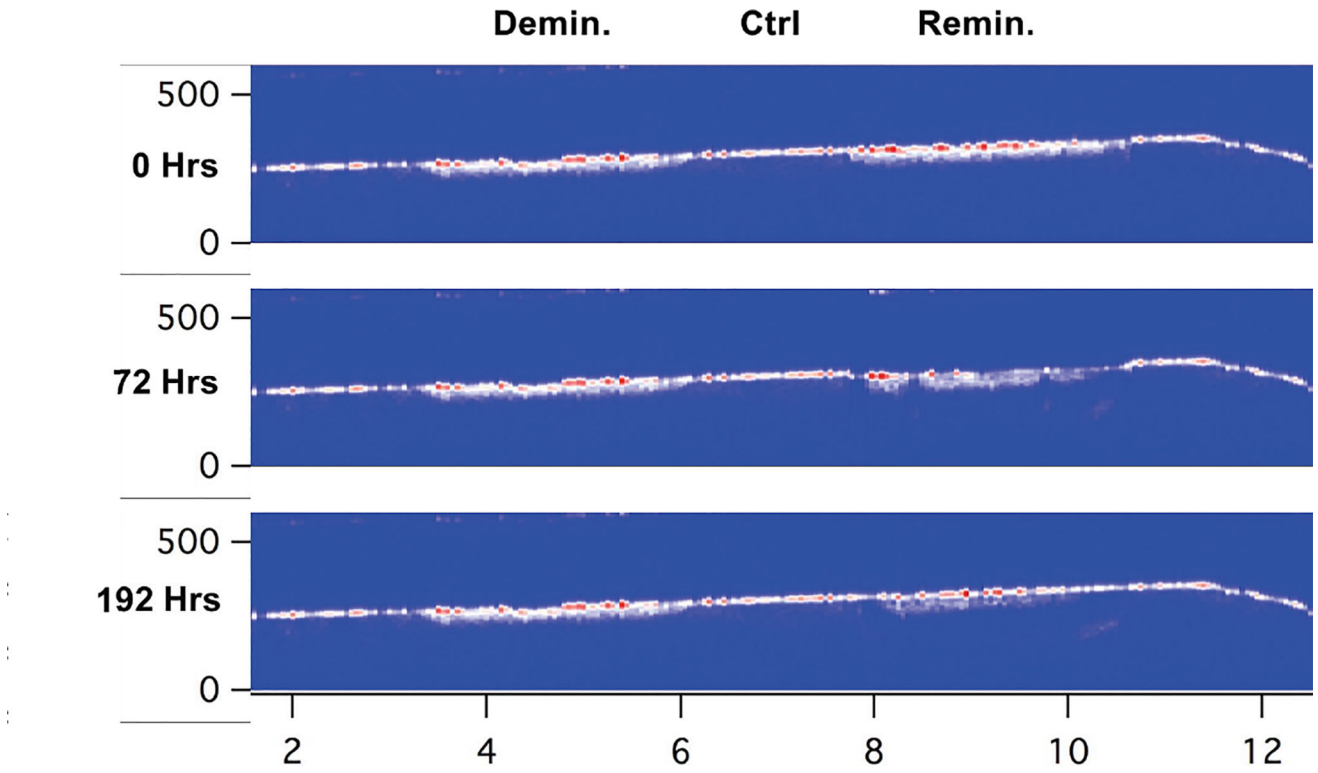

Fig. 3.

A sample PS-OCT B-scan of an enamel block at 0, 72, and 192 hours of remineralization followed by 24hrs of demineralization. Dimensions measured in μm. Note the growth of the transparent surface layer in the remineralized zone.

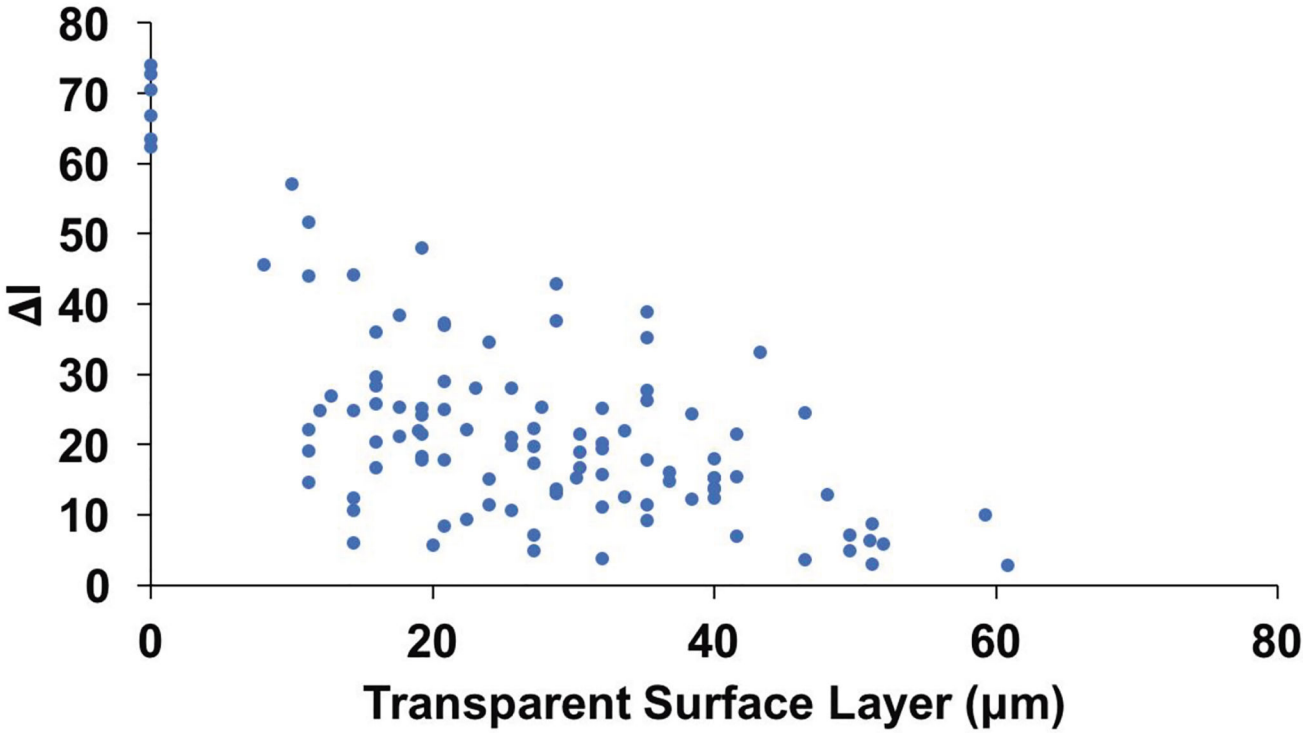

Fig. 4.

Correlation between NIR reflectance dehydration measurement and the thickness of the transparent surface layer measured by PS-OCT, $r^2 = 0.42$.